GEOPHYSICS, VOL. 71, NO. 2 (MARCH-APRIL 2006); P. B29–B40, 13 FIGS., 3 TABLES.
10.1190/1.2187709

Case History

Comparison between reprocessed seismic profiles: Seismologic and geologic data — A case study of the Colfiorito earthquake area

Eusebio Stucchi[1], Francesco Mirabella[2], and Maria Grazia Ciaccio[3]

ABSTRACT

Seismic reflection data are used to reconstruct the subsurface geologic structures below the Umbria-Marche region in Italy, a highly seismogenic area with a recent history of seismic activity (the 1997–1998 Colfiorito sequence). We reprocess three vibroseis seismic profiles (acquired in the early 1980s for hydrocarbon exploration) whose stacked sections were optimized for relatively deep oil targets. On the reprocessed seismic profile closest to the epicentral area, we construct the main reflectors to a depth of about 4 s (two-way time) and compare this interpretation with the available hypocenters of the 1997 earthquakes.

The improvements in visualizing the shallow and deep reflections provide a better correlation between the reflectors and the observed surface structures as well as a better delineation of the basement-rock geometry. We find that part of the Colfiorito sequence is localized around some of the reflectors in the reflection profile, which we interpret as related to the active normal faults that outcrop at the surface.

INTRODUCTION

Earthquake seismology and seismic reflection profiling are often used to study the earth's subsurface through different approaches and with different objectives. Despite sharing the same fundamental principles of wave propagation, these methods are seldom used jointly, even when research objectives are similar, as in the case of upper-crust investigations in regions struck by earthquake sequences.

Attempts have been made to define the geometry of seismogenic faults by acquiring near-surface seismic reflection data at the fault location (Wang, 2002) and by using reflection data previously acquired for hydrocarbon exploration (e.g., Williams et al., 1995; Boncio et al., 1998; Mirabella and Pucci, 2002; Pauselli et al., 2002; Bardainne et al., 2003; Collettini et al., 2003). Similarly, at the end of the 1990s, after the Kinki district was struck by the January 1995 Kobe earthquake [7.2 magnitude (M) on the Richter scale], the Geologic Survey of Japan and other public and scientific Japanese institutions made ad hoc seismic surveys to investigate the deep structures beneath Osaka Bay (Yokokura, 1999).

For our case study, large quantities of reflection seismic, seismologic, and structural geologic data were available in the seismically active Umbria-Marche region in Italy. Each data type contributes to the characterization of the active fault systems and provides mutual constraints. Therefore, we concentrate on the methodological aspect of comparing and integrating the outcome of various techniques and these data sets. We mainly focus on reprocessing three seismic reflection profiles acquired in the early 1980s by ENI-AGIP. These seismic lines cross a currently tectonically active area within the northern Apennines in central Italy (Colfiorito area). Between 1997 and 1998 this region underwent a long seismic crisis, characterized by six main shocks measuring $5.2 < Mw < 6.0$, all nucleated on southwest-dipping normal faults (Amato et al., 1998; Selvaggi et al., 2002; Chiaraluce et al., 2003), where MW is the moment magnitude scale. The depths investigated by the seismic lines extend beyond 4 s two-way time (twt); traveltime roughly corresponds to about 10 km depth, which is comparable with the thickness of the shallow seismogenic layer (~1–9 km below sea level; Boncio et al., 2000).

We first describe the seismotectonic setting, then the available seismic data set, and next the reprocessing we applied

Manuscript received by the Editor September 17, 2004; revised manuscript received June 7, 2005; published online March 7, 2006.
[1]University of Milan, Earth Sciences Department — Geophysics, Via Cicognara 7, 20129 Milan, Italy. E-mail: eusebio.stucchi@unimi.it.
[2]University of Perugia, Earth Sciences Department, Perugia, Italy. E-mail: mirabell@unipg.it.
[3]Istituto Nazionale di Geofisica e Vulcanologia, Via di Vigna Murala 605, 00743 Rome, Italy. E-mail: ciaccio@ingv.it.

to the three vibroseis seismic lines. We then perform a geologic line drawing of the main reflectors (bedding and faults) on the time section crossing the epicentral area of the 1997–1998 seismic sequence, integrating this information with the geologic faults (interpreted on the reprocessed seismic line) and the hypocentral locations reported in the literature. We check for a rough consistency between earthquake locations and fault geometry by working in the time domain because of the low quality of the seismic data, the uncertainty in the estimated velocity field, and the 1D velocity model used to locate at depth the recorded earthquakes.

TECTONIC SETTING

The Umbria-Marche region (central Italy) is characterized by a current tectonic extension that has been active since the upper Pliocene–lower Pleistocene (1.8–2.0 Ma). The extension is superimposed on a Miocene-Pliocene compressional tectonic phase that formed the Umbria-Marche fold-and-thrust belt (Elter et al., 1975; Pialli et al., 1998). In this area the extension (Figure 1) consists of a set of southwest-dipping normal faults (Gubbio normal fault, Colfiorito fault system, Norcia fault) that form an active fault alignment (Umbria fault system, or UFS; Barchi, 2002) bordering the northwest-southeast trend of the Quaternary Gubbio, Colfiorito, and Norcia continental basins. Seismic profiles show that at least the northern part of the UFS is antithetic to the eastward-dipping, low-angle Altotiberina normal fault (Boncio et al., 2000; Collettini and Barchi, 2002) that borders the western ridge of the Tiber valley (Figure 1).

The southwest-dipping normal faults of the UFS are Quaternary age at the base of the basin's infill and are considered active from geomorphological (e.g., Ficcarelli and Mazza, 1990; Coltorti et al., 1998; Messina et al., 1999), geologic (e.g., Lavecchia et al., 1994; Calamita et al., 1999; Barchi et al., 2000; Boncio and Lavecchia, 2000; Mirabella and Pucci, 2002), and seismological evidence (e.g., Deschamps et al., 1984; Haessler et al., 1988; Amato et al., 1998; Ekström et al., 1998; Mariucci et al., 1999; Stramondo et al., 1999; Barba and Basili, 2000). Historical seismicity data (Imax = XMCS, CPTI, 1999) and recent earthquakes [Norcia, 1979, Ms (surface-wave magnitude) = 5.9; Gubbio, 1984, Ms = 5.2; Colfiorito, 1997–1998, maximum Mw = 6.0] (Deschamps et al., 1984; Haessler et al., 1988; Deschamps et al., 2000) indicate an active stress field consistent with a geologic long-term stress field that has been active since the Quaternary (Mariucci et al., 1999).

The 1997–1998 Colfiorito seismic crisis occurred on normal faulting and has allowed a detailed characterization of the activated seismological fault segments in the investigated area. This long seismic sequence started on September 26, 1997, with two earthquakes of moderate magnitude: 5.8 and 6.0 Mw. During the sequence four additional events of 5.2 to 5.6 Mw occurred. All of the large shocks (Amato et al., 1998; Selvaggi et al., 2002; Chiaraluce et al., 2003) originated at 5 to 6 km depth and were on adjacent, parallel, northwest-trending normal faults. Figure 2 superimposes the position, focal mechanisms, and intensities of the main shocks on a structural sketch of the study area. Figure 3 shows the main tectonic features (faults and fold axes) and two geologic cross sections, depicting the subsurface geometry of the geologic structures to a depth of 2 km below sea level (bsl).

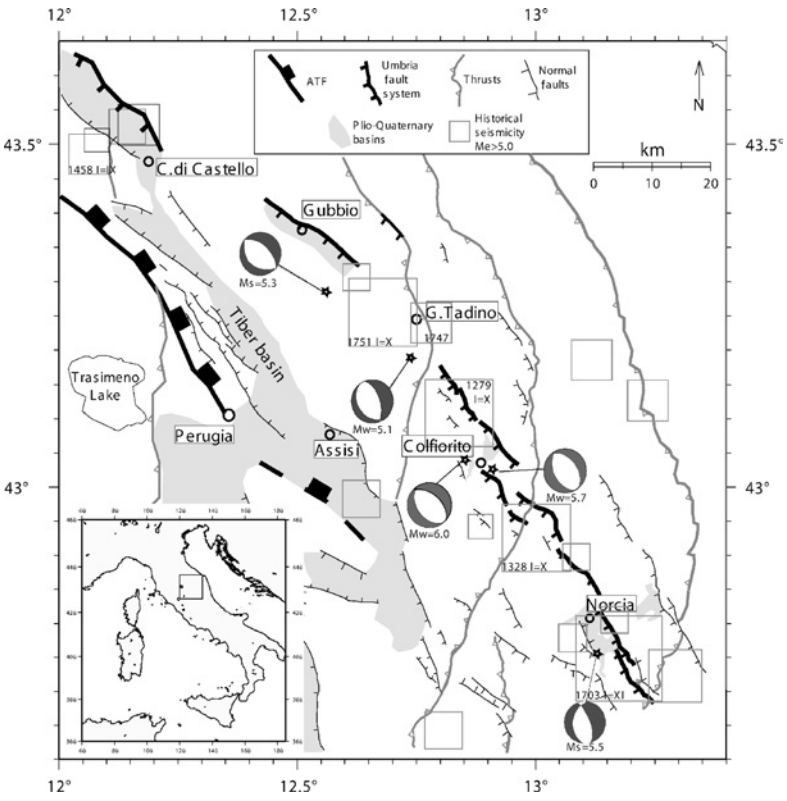

Figure 1. Schematic structural map of the Umbria-Marche region, showing the alignment of the intramontane basins along the Umbria fault system (UFS). Historical seismicity is reported from 461 B.C. to A.D. 1979 (Boschi et al., 1997). Focal mechanisms and magnitudes are for the 1997–1998 Colfiorito sequence (Ekström et al., 1998), for the 1979 Norcia earthquake (Deschamps et al., 1984), and for the 1984 Gubbio earthquake (Dziewonski et al., 1985). ATF — Altotiberina fault.

Despite the high-resolution locations of the seismic sequence, a direct connection between the activated faults at depth (Chiaraluce et al., 2003) and the outcropping normal faults (Figure 3a) is still a matter of debate, mainly because surface ruptures during the 1997–1998 seismic crisis cannot be well placed and surface breaks have been associated with only a few fault segments (Cinti et al., 2000). However, the available data indicate a strong relationship between ground deformation, the trace of the Quaternary normal faults at the surface, the subsided area, and the earthquake locations (Chiaraluce et al., 2005). This relationship suggests a connection between the surface structures and the faults activated between 1997 and 1998.

Another matter of concern regards the depth geometry of the active normal faults (i.e., listric or planar) and the relationships between the active normal faults and the preexisting compressional structures. In fact, good-quality seismic reflection profiles northwest of the study area show that another segment of the UFS (the Gubbio fault; see location in Figure 1) reactivates a

preexisting thrust at depth and that its final shape is listric (Mirabella et al., 2004). Other Quaternary normal faults in central Italy, similar to the Gubbio normal fault, have reactivated preexisting normal faults (Calamita et al., 1998; Tavarnelli, 1999; Pizzi and Scisciani, 2000; Pizzi et al., 2002). However, the Quaternary normal faults in the study area are not supposed to be the result of reactivation of preorogenic normal faults because of their morphotectonic shape (Mirabella et al., 2005). Moreover, the orientation of the thrust faults (about north-south) with respect to that of the Quaternary normal faults (Figure 3a) cropping out at the surface (about northwest-southeast) led us to believe that reactivation at depth of the thrust faults is unlikely to occur. With regard to the deep attitude of the main active faults in the Colfiorito area, no definitive data are yet available to fully define their geometry at depth. However, on the basis of the gathered data (Barchi, 2002; Mirabella and Pucci, 2002; Collettini et al., 2003; Chiaraluce et al., 2005), it seems reasonable to consider a variation of dip with depth from about 55° at the surface (Figure 3b) to about 40° at earthquake nucleation depths (i.e., ~6 km). Such a geometry is also characteristic of the northwestern Gubbio normal fault, which also belongs to the UFS (Mirabella et al., 2004).

AVAILABLE SEISMIC DATA

At the beginning of the 1980s, many oil companies, particularly ENI/AGIP, extensively explored the study area for hydrocarbon exploration. Such activity produced an approximately 300-km-long grid of seismic reflection profiles and borehole data. The recorded reflection traveltime corresponds with depths to 8 to 10 km. This data set, made available only recently, provides an independent data source for the geometric reconstruction of the subsurface geologic structures. In particular, it allows for the geometric reconstruction of currently active faults (Boncio et al., 1998; Pauselli et al., 2002; Collettini et al., 2003; Mirabella et al., 2004), which can be compared with the main shock and aftershock distribution. Moreover, the CROP03 seismic reflection profile acquired in the Italian deep-crust exploration project is also available; it has shown interpretable seismic data down to tens of kilometers Pialli et al., 1998). Three vibroseis seismic lines, recorded in crucial areas — for example, in correspondence with hypocenter locations or where there was surface evidence of major faults — were selected from the ENI/AGIP data set (lines GT-1, CF-1, and CF-2). Figure 2 shows the trace of the seismic profiles, and Table 1 gives the acquisition parameters.

Seismic exploration in the Apennines is very challenging (Bertelli and Mazzotti, 1998; Bertelli et al., 1998; Mazzotti et al., 2000) because the complex tectonic regional setting and the characteristics of outcropping formations (especially fractured carbonate rocks) greatly hamper seismic signal penetration. Moreover, the topography of the area greatly increases the difficulty of the statics computations needed for these very heterogeneous and composite surface layers. It also causes accessibility problems, especially for vibroseis trucks. Furthermore, these data were processed in the early 1980s with the technology available at that time and with relatively deep oil targets as the main objectives. Thus, the margins for

Table 1. Acquisition parameters.

Parameter	Data
Date recorded	June 1983
Source type	Vibroseis
Sample rate	4 ms
Record length	6 s
Low-cut filter	12 Hz
Low-cut slope	18 dB/octave
High-cut filter	88 Hz
High-cut slope	78 dB/octave
Notch filter	50 Hz
Instruments	Coba II
S. P. interval	100 m
Number of vibrators	4
Number of sweep/V. P.	16
Sweep frequency	17–69.5 Hz
Sweep length	10 s
Geophone pattern	Linear 24 × 100 m
Geophone type	SM4B 14 Hz
Spread type	Off end
Spread configuration	2800 m–450 m-X
Number of groups	48

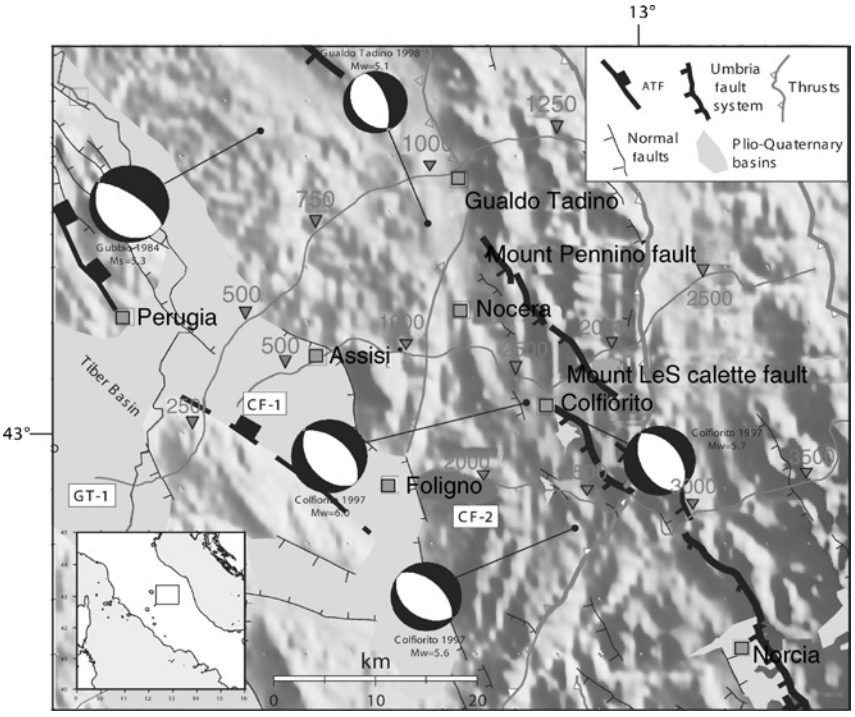

Figure 2. Location of vibroseis profiles GT-1, CF-1, and CF-2 on a schematic structural sketch of the area. The focal mechanisms and intensities of the main shocks are reported also (Wessel and Smith, 1995).

improving the quality of the final seismic sections are wide: today's processing algorithms can be focused on the optimal definition of the fault systems, both at depth and across very-near-surface layers.

Reprocessing seismic data

On the basis of previous experience (Mazzotti et al., 2000) and considering the outcome of specific tests carried out on vibroseis data subsets, we were able to develop an unconventional processing sequence tailored to the specific problems we encountered. Table 2 shows the sequence flowchart; the most important steps are described below.

Typical examples of raw, common-source gathers are shown in Figure 4. Most of the source records have similar amplitude spectra (Figures 5a–5c) in which many useful frequencies were considerably attenuated by applying a 50-Hz notch filter directly to the field data. An original spectrum, found in a few isolated records, is shown in Figure 5d. After building the geometry database and signal dephasing (with the Coba II instrument response), a semiautomatic procedure based on first-break energy, and the frequency content of each trace helped the editing of noisy traces. The procedure was applied in a restricted way; to completely remove noisy traces, we performed a visual inspection and manual editing in different domains [common source, common offset, common midpoint (CMP)].

One of the greatest difficulties we dealt with was statics computation. In fact, in addition to the topography (Figure 6b) and velocity variation in the near-surface layers, the vibrocorrelation precursors made the first-break picking for refraction statics a sensitive operation (Figure 4). We used

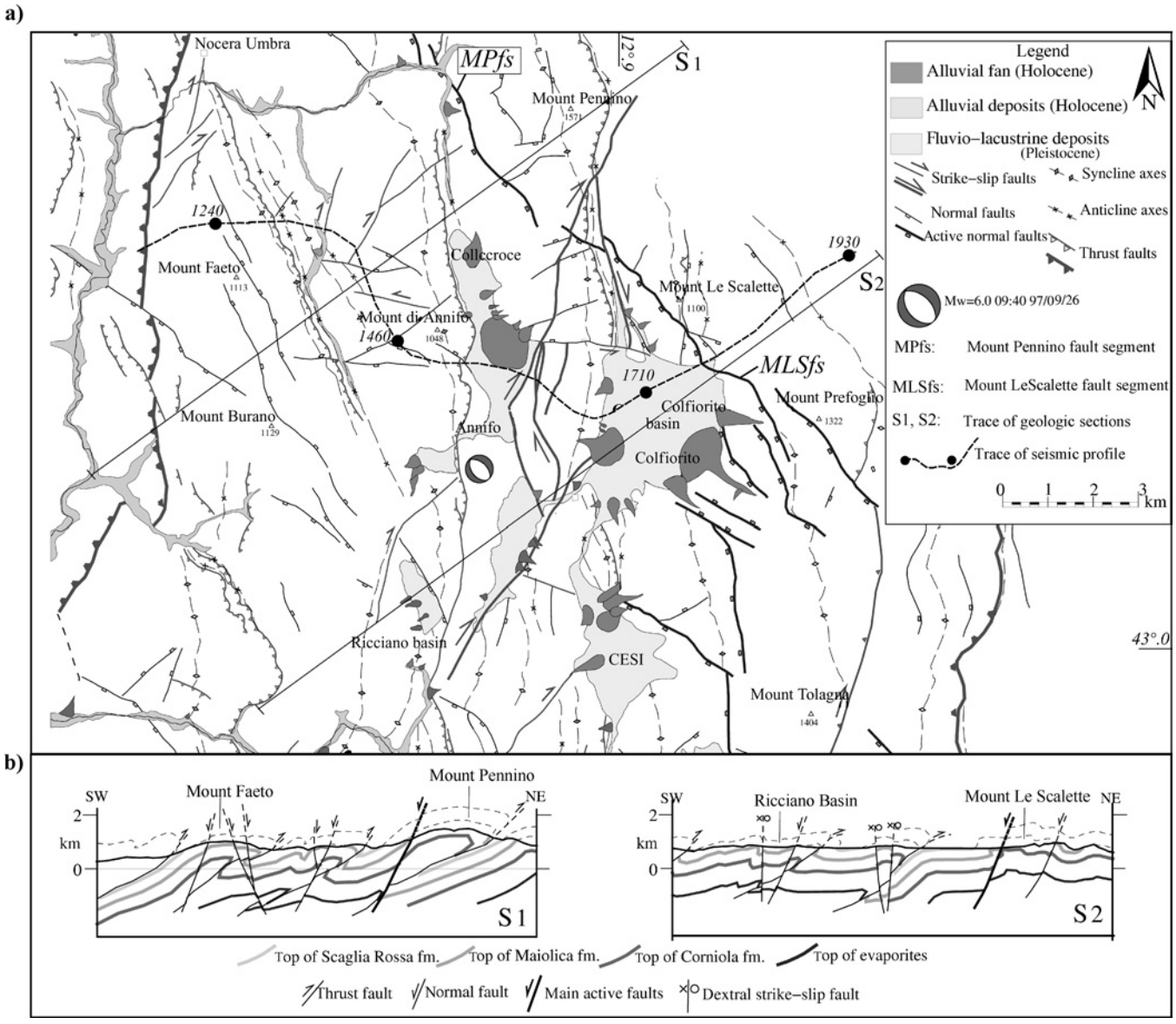

Figure 3. (a) Geologic sketch of the Colfiorito area, derived from 1:10.000-scale field mapping, showing the main tectonic features (faults and fold axes) and the position of the continental deposits. (b) Geologic cross sections, showing the subsurface geometry of the geologic structures to a depth of 2 km below sea level. The position of the 6.0 Mw main shock and the CF-1 reprocessed seismic profile are also shown. Modified after Chiaraluce et al. (2005).

both in-house-developed codes (Zanzi, 1996) and industrial software (ProMAX), and we considered only a single refractor layer solution (refractor offset ranges from 500 to 2000 m). Figure 7 shows the refraction statics application on a constant-velocity stack ($V = 4000$ m/s) between 0 and 1.3 s (line CF-2). Note the different shapes of the reflections after the correction, an important point when tracing the fault system to shallow times. Such shapes make it easier to match surface geologic observations with reflection data.

To increase the S/N ratio on the stacked section, especially for shallow reflections, we used optimum slalom-line sorting. The crooked-line binning procedure adopted gives us the flexibility to test different slalom-line sorting criteria. Our experience (Mazzotti et al., 2000) showed that the near-offset track yields, on average, the best results. Therefore, we chose this track and avoided an excessively crooked definition on the final profiles. Figure 6a shows an example of the slalom-line sorting definition. The black and white points represent the receiver and source positions, respectively, while the source-receiver midpoints used in the binning procedure are displayed in color as a function of offset. The final track, the magenta line in Figure 6a, lies close to the green midpoints that correspond to short-offset traces.

To further reduce the incoherent noise in the prestack level, we applied a soft frequency-offset deconvolution in the common-offset domain. We used null traces to pad missing data because of trace editing or lack of acquisition.

The loop from the velocity analysis to the stack (Table 2) for deep (>1.5 s) and shallow (<1.5 s) data was repeated independently. Each sequence was optimized, especially in those steps requiring interaction such as velocity analysis and residual statics correction. Velocity analysis was carried out first with the constant-velocity stack method and was then refined with the semblance tool. The residual statics correction was computed with the stack maximum power algorithm, carefully defining the horizons for both deep and shallow cases. A time-variant filter was applied on the final stack, using a gradually narrowing band-pass frequency interval from shallow to deeper recording times.

Predictive deconvolution was attempted in the prestack domain. However, the results were not as good as expected, probably because of the noise level still present in the data. Therefore, we applied predictive deconvolution after stacking to take advantage of the incremented S/N ratio. Finally, we applied frequency-offset deconvolution, using the same parameters as for the common-offset domain.

Examples of the improvements achieved in the final seismic images can be seen in Figures 8–10. These figures show the same stack segment of lines CF-2, GT-1, and CF-1 before and after the reprocessing sequence. In the reprocessed profiles (Figures 8b, 9b, and 10b), the increased lateral continuity of the deep reflections is evident and allows an interpretation of their geometry at depth with respect to the previous sections, where only sparse reflectors can be observed. Moreover, the events at shallow times are clearly visible and well delineate the structures close to the surface. These structures can now easily be correlated with geologic field observations, outcropping lithologies, and fault segments. The increased resolution of the geologic structures on the reprocessed profiles (Figures 8b, 9b, and 10b) leads to a clearer image of some of the key reflectors and main

Table 2. Processing sequence, optimized for $t < 1.5$ s and $t > 1.5$ s.

Data loading	
Geometry installation	
Dephase	
Trace editing and filtering	
Band-pass filter = 14-16-68-75 Hz	
Refraction statics	
Prestack frequency-offset deconvolution in common offset	
Horizontal window length = 10 traces	
Number of filter samples = 4	
Time window length = 400 ms	
Time window overlap = 100 ms	
CMP binning	
Automatic gain control (1200 ms)	
Velocity analysis	
NMO correction	
Residual statics	
Stack	
Time-variant filter	
0–1100 ms	14-16-60-65 Hz
900–3600 ms	14-16-30-34 Hz
3400–6000 ms	14-16-26-29 Hz
Deconvolution	
30 ms prediction distance	
60 ms operator length	
Frequency-offset deconvolution	
same parameters as prestack frequency-offset deconvolution	
Display	

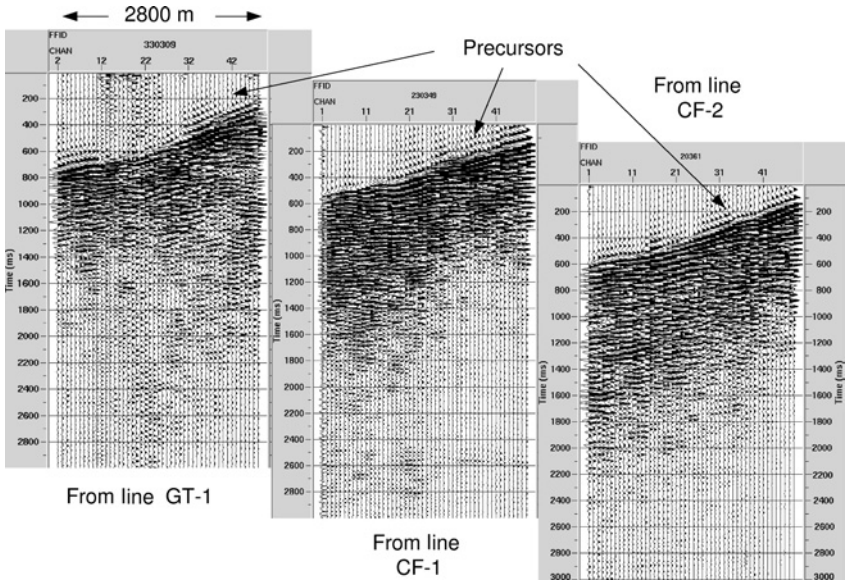

Figure 4. Example of raw shot gathers (one from each seismic line). Data quality is similar for the three seismic profiles, and the low S/N ratio of the whole data set is evident. Note the precursors of the autocorrelation.

tectonic structures within the Umbria-Marche stratigraphy, as is discussed for seismic line CF-1 next.

LINE DRAWING OF MAIN REFLECTORS

The reprocessed seismic profile CF-1 (Figures 10 and 11) shows remarkable improvements, particularly for the deep reflections corresponding to the top of the Permo-Triassic basement. These reflections reside at the base of a sedimentary sequence comprised of Triassic evaporites (Anidriti di Burano Formation; Martinis and Pieri, 1964) and overlain by a lower Jurassic–early Oligocene carbonate multilayer (Umbria-Marche stratigraphic sequence; Cresta et al., 1989). The reflectors of the basement rocks are characterized by strong and slightly discontinuous reflections. They deepen and step toward the east from about 2.3 s twt at about CMP 800 to approximately 3.5 s twt near CMP 1240. We relate these reflections to the involvement of the basement in the main thrust sheets of the Umbria-Marche Apennines, as recognized on seismic profiles in this region (e.g., Barchi et al., 1998; Pialli et al., 1998; Pauselli et al., 2002). Other similar reflections, related to the top of the basement rocks, are located at about 3 s (twt) near CMP 2040 and eastward (Figure 11a).

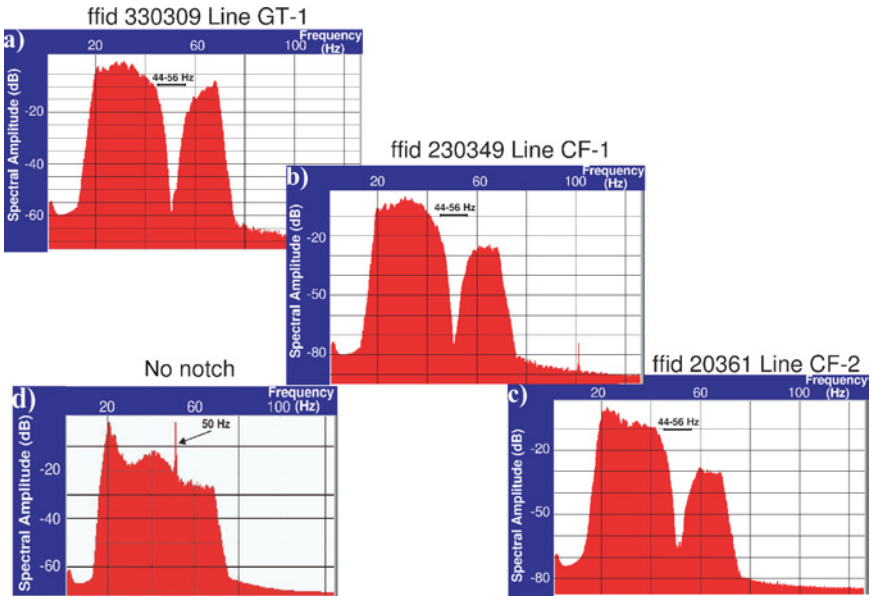

Figure 5. Amplitude spectra of the common source records in Figures 4a–4c. Note the deep trough resulting from the field application of the 50-Hz notch filter. Unfortunately, the full vibroseis bandwidth was recorded only in selected isolated gathers (d).

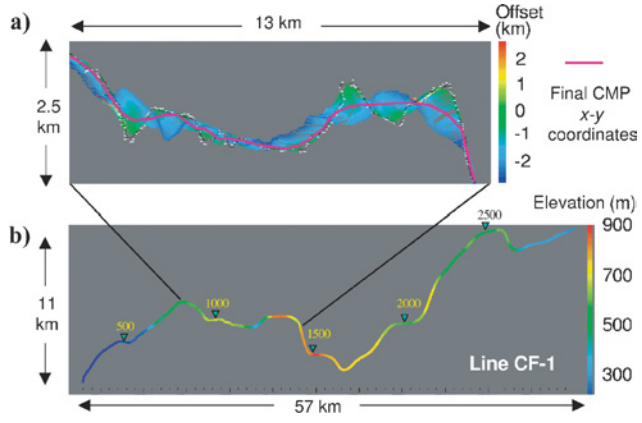

Figure 6. (a) The crooked-line acquisition and (b) variations in topography that complicated reprocessing. Elevation differences of 600 m for (b) line CF-1 and even more for the CF-2 (1400 m) and GT-1 (800 m) profiles are observed. The final track selection [(a), magenta line] is close to the short-offset midpoints in green.

The correlation of the shallower reflections (up to about 1.5 s twt) with surface geology allowed us to recognize some reflections of the upper part of the carbonate multilayer, especially the Marne a Fucoidi Formation (Aptian-Albian in age). This formation is a marly interval within the carbonate succession and is usually easily recognizable and widely used as a key horizon when interpreting the seismic profiles of the region (e.g., Barchi et al., 1998). Near the surface, up to about 1 s twt, several reflectors belonging to the carbonate multilayer are recognizable. Their attitudes reflect the geometry of the geologic structures at the surface. In particular, the reflections of the carbonates belonging to the main anticlines of the area (e.g., Mt. Subasio and Mt. Faeto) are well imaged (Figure 11a).

The profile of Figure 11 shows a reflector alignment at about 2.0 to 2.2 s twt, from CMP 1240 to CMP 1320, below Mt. Faeto in the central part of the section. In our interpretation, this well-aligned package of reflections belongs to carbonate rocks downthrown by a southwest-dipping normal fault that we interpret to be deep evidence of the main southwest-dipping active normal faults corresponding to the Mt. Le Scalette–Mt. Pennino fault segments at the surface (see Figure 3).

Because the seismic profile is crooked, its track between CMPs 1360 and 1640 runs almost parallel to the normal fault segments (see Figures 2 and 3). Hence, in this part of the section the trace of the normal fault is nearly planar. The trace geometry of the normal fault in the seismic section is thus a multisegmented line composed of (1) an upper part from the surface down to about 1.5 s twt; (2) an almost flat part at about 2 s twt, and (3) a southwest-dipping part from 2 to about 2.5 s twt. The trace in the central part is shown by a dashed line because, notwithstanding the improvements obtained from the new reprocessing sequence (see Figure 10), the lack of signal in this area does not allow a direct connection between the reflectors at depth and the reflectors at the surface. This can be observed in Figure 11b, which shows the corresponding unmarked seismic section. The horizontal–vertical-scale ratio of Figure 11a is usually used for commercial seismic profiles of the area, while in Figure 11b the time scale is doubled with

respect to Figure 11a to better display the recovered seismic signal.

PLACEMENT OF HYPOCENTERS ON THE SEISMIC SECTION

To compare earthquake locations (in depth) with the geometries inferred from seismic reflection profiles (in time), a common domain (time or depth) is required. The optimal procedure would be (1) estimate an optimal 3D velocity field from seismic and seismological observations, (2) locate in depth the earthquake foci honoring the lateral/vertical velocity variations of the velocity model, and (3) depth-migrate the seismic reflection data with the same velocity field.

This procedure has not been carried out yet because the quality of the seismic data and the uncertainty of the estimated velocity field preclude high-quality, reliable depth images. Indeed, despite the enhanced S/N ratio at the end of the reprocessing sequence (Figues 8–10), the still-present noise and the limited maximum offset (<3 km) do not allow the exploitation of more powerful tools, such as migration velocity analysis, to build an accurate velocity field at depths greater than 4 to 4.5 km. Moreover, the classical hypocenter uses a 1D velocity field (layer-cake type, the velocity increasing with increasing depth) derived by seismological observations only.

While the steps delineated above are being completed, we perform a preliminary time-domain correlation between seismological observations and seismic data to check whether a rough match exists between the geologic structures indicated by reflection seismic and hypocenter locations. To this end we use the seismological and seismic information independently and proceed as follows.

First, hypocenters that were depth-located using a seismological 1D velocity field are time-converted using the same 1D

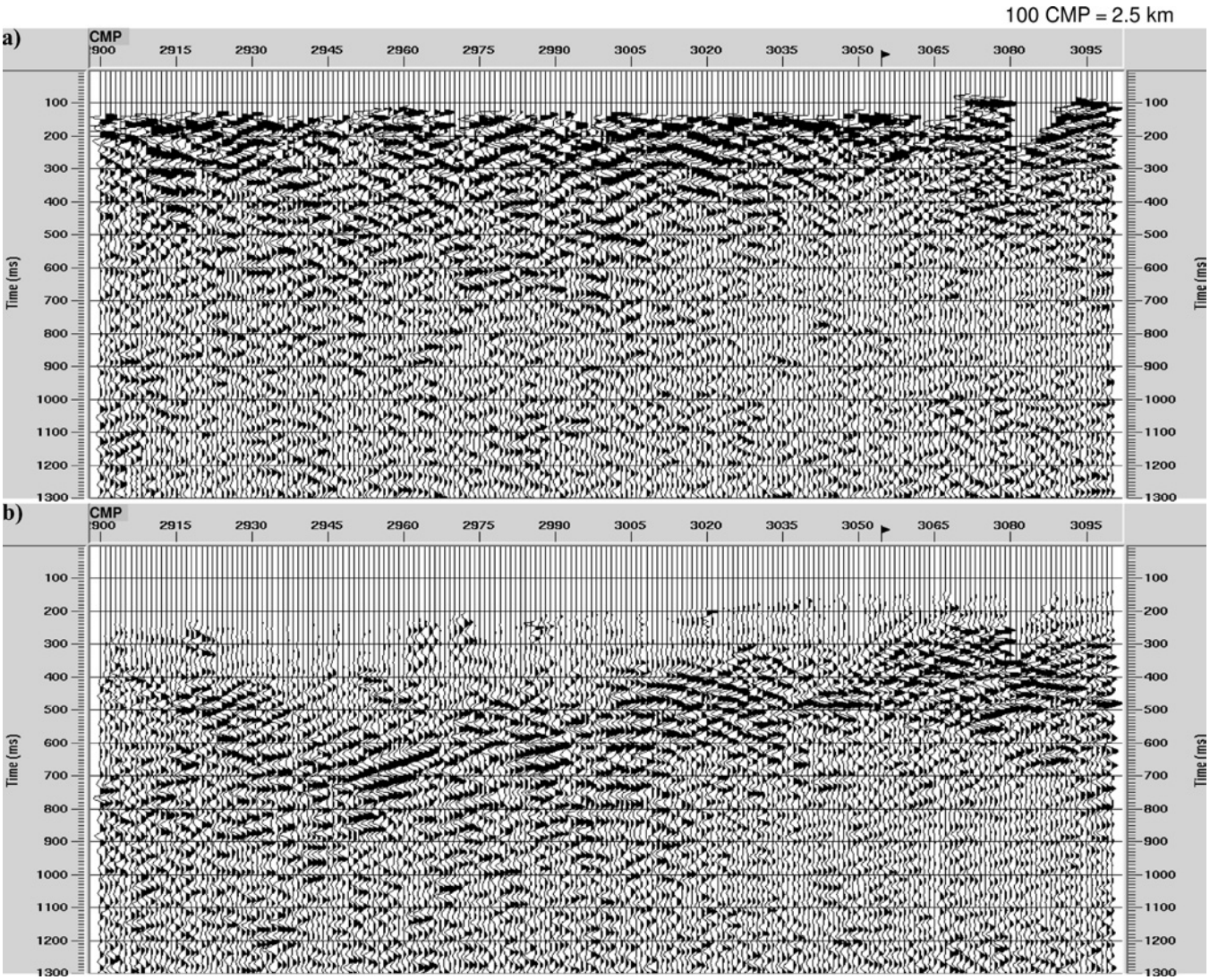

Figure 7. Constant-velocity stack ($V = 4000$ m/s) of the CF-2 profile, showing the effects (a) without and (b) with refraction statics applied. The different reflector geometries observed after the statics corrections highlight the importance of this processing step in the area. The CMP spacing is 25 m, for a total display length of 5 km.

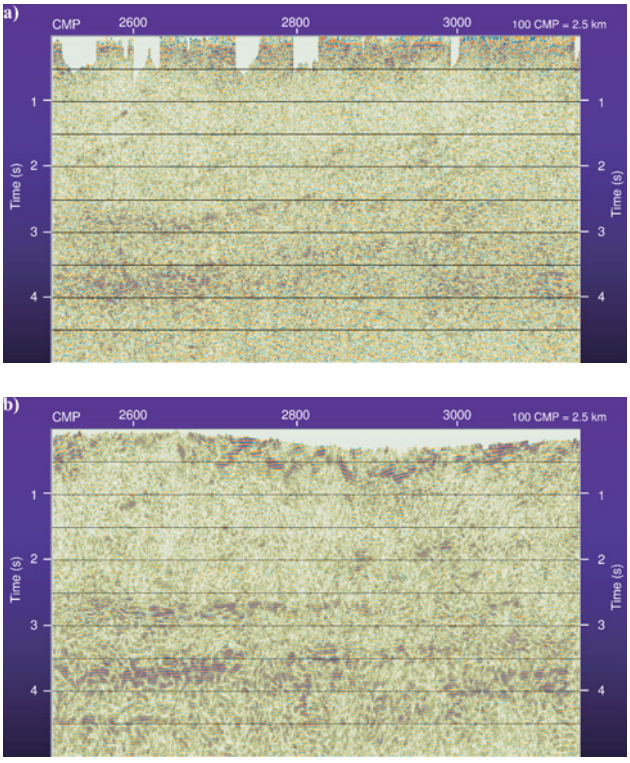

Figure 8. Portion of the CF-2 profile (~17 km long), showing the reprocessing results for this line (a) before and (b) after reprocessing.

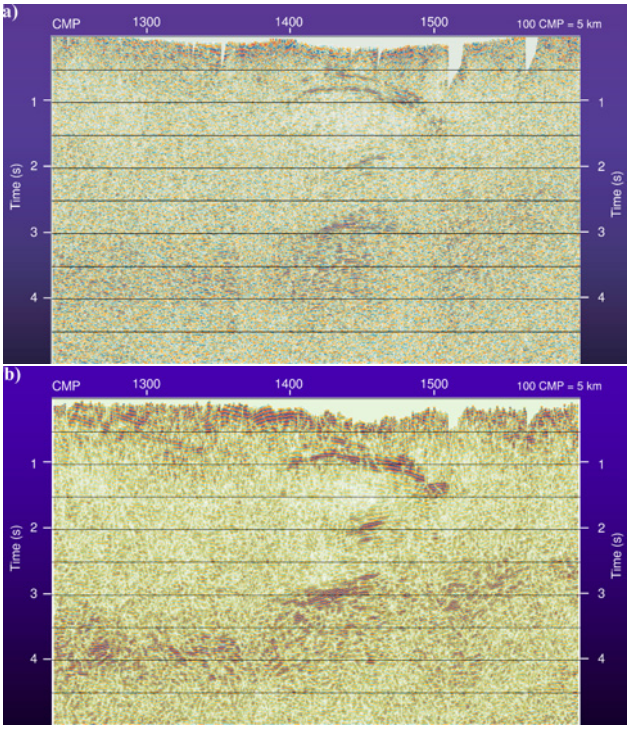

Figure 9. Portion of the GT-1 profile (~17 km long), showing the reprocessing results for this line (a) before and (b) after reprocessing In this case the CMP interval is 50 m because an interleaving procedure was used in binning the midpoints.

velocity field. Second, the time locations of the earthquake foci are projected onto the nearest seismic stack time section along the mean strike of the geologic structures.

When completing these two location steps, we make errors, especially concerning the lateral position of the seismic structures (Yilmaz, 1988; Gray et al., 2001; Robein, 2003) and earthquake events. Nevertheless, because of the uncertainty in estimating the 3D velocity field to be used in the optimal procedure outlined above, it is worthwhile to check this preliminary and approximate solution to find any consistency that may exist between these two kinds of information.

CORRELATION WITH SEISMOLOGICAL DATA: EARTHQUAKE LOCATIONS

Various and different seismological studies of the 1997–1998 earthquakes have defined the faulting mechanisms, the aftershock distribution, and the at-depth geometry of the activated fault (Amato et al., 1998; Olivieri and Ekström, 1999; Cattaneo et al., 2000; Deschamps et al., 2000; Chiarabba and Amato, 2003). These data were recorded in the epicentral area with a dense, 3-component seismic network of 29 digital stations, deployed from the morning of September 26, 1997, until November 3, 1997 (Deschamps et al., 2000), and by a permanent seismic network. The 1997–1998 seismic sequence is complex and is characterized by several thousands of aftershocks (Chiaraluce et al., 2003). However, recently published data show that a detailed integration of seismological and geologic information can help to match the geologic

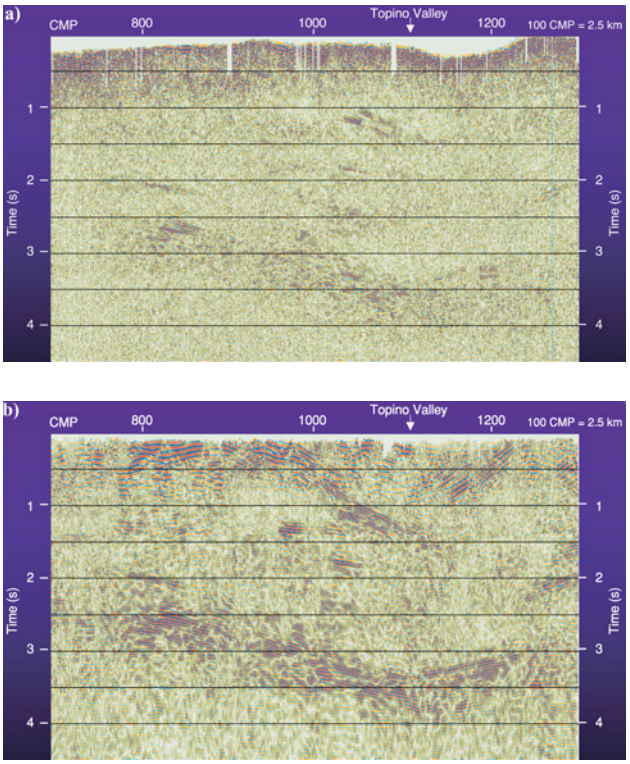

Figure 10. Detail of the CF-1 profile (~15 km long), showing the reprocessing results for the line close to Colfiorito (a) before and (b) after reprocessing.

structures with the activated fault segments (Chiaraluce et al., 2005).

Building upon these indications, we chose to project onto the seismic section the closest main shock (event of 6.0 Mw occurred on September 26, 1997, at 9:40 a.m.) and a group of aftershocks that were either close to the seismic profile or to the main shock and with a depth greater than 3 km. We selected this depth because in this part of the sequence the aftershocks shallower than 3 km are related to a secondary shallow strike-slip event (4.5 Mw) that occurred on October 16, 1997, at about 1 km depth located very near CMP 1600 (Chiaraluce et al., 2003; Chiaraluce et al., 2005). We used 158 earthquake locations (Selvaggi et al., 2002) obtained by the Hypoinverse location code (Klein, 1989) using the 1D velocity model derived from the minimization of P- and S-wave residuals on the whole data set (Kissling et al., 1994; see Table 3 for the velocity model).

Figures 12b and 12c show two vertical cross sections, *AA′* and *BB′* (with centers 12.805E-43.077N and 12.893E-43.045N, respectively), representing the estimated seismicity at depth in a range of ±0.5 km around the vertical planes defined by lines *AA'* and *BB'* in Figure 12a. Figure 13 shows the estimated vertical and horizontal errors for the whole sequence. From the histograms, we can determine a very small mean horizontal and vertical error of 0.5 and 0.75 km, respectively.

To check for consistency between seismological and seismic data, we reconverted the depths of the selected earthquakes (Figure 12a) to time with the same 1D velocity model of Table 3. The earthquakes were then projected on the CF-1 profile (see Figure 11a).

Since the main strike of the active faults is northwest-southeast (about N130°–150°), inferred by both focal solutions (e.g., Chiaraluce et al., 2003) and surface geologic data (e.g., Barba and Basili, 2000; Mirabella and Pucci, 2002; Chiaraluce et al., 2005), the earthquakes were projected following the mean strike of the active normal faults (i.e., along a N145° line). This direction is also consistent with rupture directivity data, which indicate a northwest directivity of the plotted main shock (Pino and Mazza, 1999).

In the time domain the projected events occur at a depth ranging from 1.3 to 3.5 s twt. Considering the distortion introduced by the crooked line (between CMPs 1360 and 1640, the seismic profile is approximately parallel to the strike of the normal faults), the projected hypocenters are roughly aligned along a southwest-dipping surface. Some of them are located near a group of reflections that we interpret as the expression at depth of the active normal faults outcropping at the Mount Le Scalette–Mount Pennino fault segments.

DISCUSSION

The study area is characterized by a well-documented historical and instrumented seismicity, mainly concentrated along a relatively shallow layer affecting the upper crust. In this seismogenic block, the Colfiorito sequence is confined within the first 8 to 9 km, the main shocks occurring at about 6 km depth and rupturing southwest-dipping normal faults above the Phillitic Permian-Triassic basement (Barchi, 2002; Mirabella and Pucci, 2002; Chiaraluce et al., 2003, Chiarabba and Amato, 2003; Collettini et al., 2003; Miller et al., 2004). In this area the depths investigated by the seismic reflection lines are comparable with the thickness of the shallow seismogenic layer, extending beyond 4 s (twt) — roughly corresponding to about 10 km.

Figure 11a highlights that the projected seismicity is roughly localized around a surface that we interpret as the at-depth continuance of the alignment of Mount Le Scalette–Mount Pennino southwest-dipping normal faults that many authors indicate as the surface expression of the active faults of the area (e.g., Meghraoui et al., 1999; Barba and Basili, 2000; Barchi, 2002; Mirabella and Pucci, 2002; Chiaraluce et al., 2005). The results shown in Figure 11a pertain to the time domain, not to the depth domain, which would be more natural. This choice is related mainly to the low-reflection seismic data quality and the uncertainty in the velocity-field estimation. Moreover, the strong lateral velocity variations in this geologically complex area require a more so-

Table 3. 1D velocity field.

Depth (km)	Velocity (km/s)
1–0	3.65
0–1	3.80
1–2	4.86
2–3	5.17
3–4	5.37
4–5	5.57
5–6	5.73
6–8	5.89
8–10	6.22

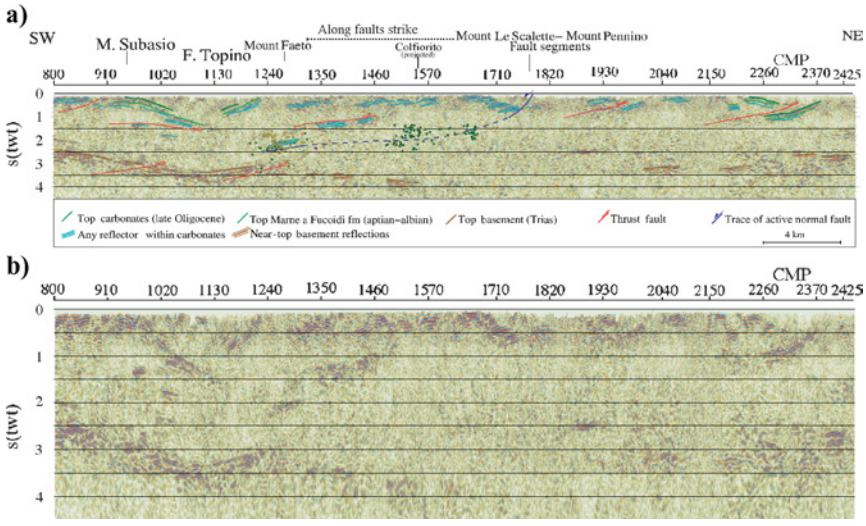

Figure 11. (a) Reprocessed CF-1 seismic profile (time domain), with a line drawing of the main reflectors and the position of earthquakes with depth greater than 3 km. The main shock is shown in magenta. (b) The reprocessed and unmarked CF-1 seismic profile, in which the time scale has been doubled with respect to (a) to better illustrate the recovered seismic signal.

phisticated approach for earthquake location at depth than the adopted 1D velocity procedure. With the raw data, the 1D velocity field provides a mean error of ±0.75 km in the hypocenter's depth, as indicated by the histogram in Figure 13. This error corresponds with a mean time difference on the order of ±270 ms. Similarly, a velocity variation of ±10% on the values listed in Table 3 implies a mean hypocenter time displacement of −220 ms and +270 ms, respectively (the maximum error occurring at the deepest event: −340 ms and +420 ms). These figures, along with the uncertainty resulting from the additional horizontal error (mean value ~0.5 km, i.e., 20 CMPs Table 1), illustrate the need for an accurate velocity field to better constrain the hypocenter location and to migrate the seismic data. Indeed, attempts to apply Kirchhoff depth migration to the stacked section gave an unsatisfactory result using a smoothed version of the stacked velocity field or the velocity field derived from interpretation.

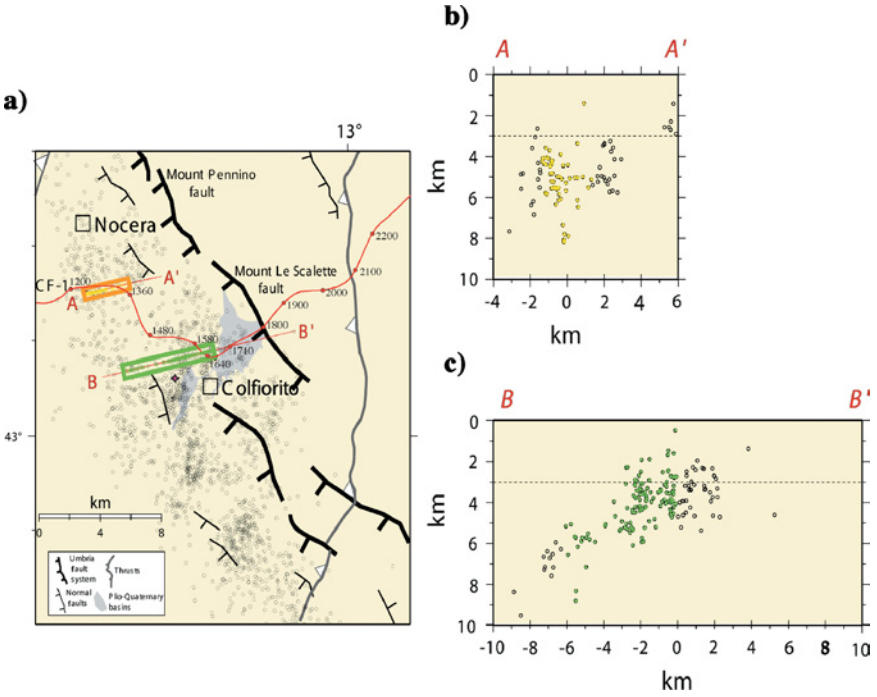

Figure 12. (a) Earthquake map and depth sections along lines (b) *AA'* and (c) *BB'*, showing the epicenter and some estimated hypocenter locations of the Colfiorito seismic sequence. The earthquakes in the green and yellow boxes (a) are also displayed in (b) and (c) in color. Those with depths greater than 3 km are projected onto the seismic stack section CF-1 parallel to the main structures' orientation. The main shock of the September 26, 1997, earthquake is shown in magenta.

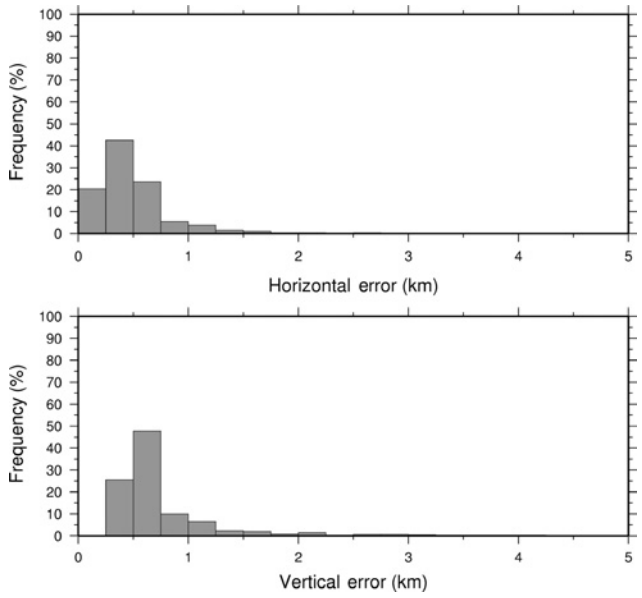

Figure 13. Histograms showing the estimated vertical and horizontal positioning errors for the whole sequence.

CONCLUSIONS

Our study shows that the characterization of an active fault system in seismically active regions can benefit from a multidiscipline approach, especially where seismic data, seismological data, and geologic knowledge are available. In fact, the enhanced quality of the final seismic sections improves characterization of the subsurface setting both at depth (in two-way time) and near the surface and allows for a better constraint of the active faults image.

Indeed, the selected main shock and aftershocks projected onto the seismic stacked time section of the closest reprocessed profile are roughly aligned along a southwest-dipping surface and are located near a group of reflections interpreted as the expression at depth of the active normal faults outcropping at the surface. Moreover, the hypocenters are located above the reflector corresponding to the top of the Phillitic Permian-Triassic basement, indicating enucleation possibly within the triassic evaporites. The consistency between seismic, geologic, and seismological information is checked in the time domain, not in the more natural depth domain, as a result of the low reflection seismic data quality, the 1D velocity model used for earthquake location at depth, and the uncertainty in the velocity field estimation.

Thus, we believe that whenever seismic reflection profiles are available in seismogenic areas, they should be used in conjunction with seismological and geologic data to better characterize the active fault system. The only limitation in using reflection sections is a sufficient depth of penetration of the seismic signals in relation to the depths of the seismogenic structures. In many instances this is not a problem, since upper-crust earthquake foci are well within the depth range of industrial seismic reflection profiles, and since accurate reprocessing efforts can provide excellent information. Only deep seismicity regions (>15 km) are precluded by the application of common industrial reflection seismic profiles, although in the recent past several deep-crust exploration projects such as the Italian CROP project have shown interpretable seismic data down to some tens of kilometers, further deepening the

reach of reflection seismology. The Colfiorito site meets all requirements regarding the availability of seismic, seismological, and geologic data, and this convenient situation is common to other seismogenic areas, such as the region of S. Giuliano di Puglia in southern Italy. Here, an earthquake struck in October 2002, and we soon hope to apply our multidisciplinary approach to the available data.

ACKNOWLEDGMENTS

This work was carried out within the auspices of two projects: Development and Comparison Between Methodologies for the Evaluation of Seismic Hazard in Seismogenic Areas: Application to the Central and Southern Apennines (Gruppo Nazionale per la Difesa dai Terremoti) and Geophysical, Geologic, and Geochemical Investigations in the Seismogenic Area of Colfiorito: Synthesis of an Integrated Model (Ministero dell' Istruzione dell' Universitá e della Ricerca).

We would like to thank ENI/AGIP for data availability and are very grateful to A. Mazzotti, L. Zanzi, and M. Barchi for their continuous suggestions and encouragement. Thanks are also given to A. Amato, M. Cocco, C. Chiarabba, and P. Montone for useful discussions.

The processing was carried out with Landmark Graphics' ProMAX software. Some of the figures were produced using Generic Mapping Tools.

REFERENCES

Amato, A., R. Azzara, C. Chiarabba, G. B. Cimini, M. Cocco, M. Di Bona, L. Margheriti, S. Mazza, F. Mele, G. Selvaggi, et al., 1998, The 1997 Umbria-Marche, Italy, earthquake sequence: A first look at the main shocks and aftershocks: Geophysical Research Letters, **25**, 2861–2864.

Barba, S., and R. Basili, 2000, Analysis of seismological and geologic observations for moderate-size earthquakes: The Colfiorito fault system (central Apennines, Italy): Geophysical Journal International, **141**, 241–252.

Barchi, M., 2002, Lithological and structural controls on the seismogenesis of the Umbria region: Observations from seismic reflection profiles: Bollettino della Società Geologica Italiana special volume 1, 855–864.

Barchi, M. R., A. DeFeyter, M. B. Magnani, G. Minelli, G. Pialli, and M. Sotera, 1998, The structural style of the Umbria-Marche fold and thrust belt: Memorie della Società Geologica Italiana, **52**, 557–578.

Barchi, M., F. Galadini, G. Lavecchia, P. Messina, A. Michetti, L. Peruzza, A. Pizzi, E. Tondi, and E. Vittori, 2000, Sintesi delle conoscenze sulle faglie attive in Italia centrale: Parametrizzazione ai fini della caratterizzazione della pericolosità sismica: Gruppo Nazionale per la Difesa dai Terremoti (GNDT).

Bardainne, T., G. Sénéchal, and J. R. Grasso, 2003, Study of a gas field fracturation based on induced seismicity in 3D seismic data: European Geophysical Society/American Geophysical Union/European Union of Geosciences Joint Assembly Geophysical Research Abstracts, **5**, 06453.

Bertelli, L., and A. Mazzotti, 1998, Planning and acquisition of the NVR Crop, 03 seismic profile: Memorie Società Geologica Italiana, **52**, 9–21.

Bertelli, L., P. Storer, and A. Mazzotti, 1998, Processing strategies for the NVR Crop, 03 seismic profile: Memorie Società Geologica Italiana, **52**, 23–31.

Boncio, P., and G. Lavecchia, 2000, A geologic model for the Colfiorito earthquakes (September-October 1997, central Italy): Journal of Seismology, **4**, 345–356.

Boncio, P., F. Brozzetti, and G. Lavecchia, 2000, Architecture and seismotectonics of a regional low-angle normal fault zone in central Italy: Tectonics, **19**, 1038–1055.

Boncio, M., F. Ponziani, F. Brozzetti, M. Barchi, G. Lavecchia, and G. Pialli, 1998, Seismicity and extensional tectonics in the northern Umbria-Marche Apennines: Memorie Società Geologica Italiana, **52**, 539–555.

Boschi, E., E. Guidoboni, G. Ferrari, G. Valensise, and P. Gasperini, 1997, Catalogo dei Forti terremoti Italiani (CFTI) dal 461 a.c. Al 1990: Istituto Nazionale di Geofisica-Storia Geofisica Ambiente.

Calamita, F., M. Coltorti, P. Pieruccini, and A. Pizzi, 1999, Plio-Quaternary structural and geomorphological evolution from the Umbro-Marchean Apennines to the Umbrian Pre-Apennines and the Adriatic coast: Bollettino della Società Geologica Italiana, **118**, no. 1, 125–139.

Calamita, F., A. Pizzi, A. Ridolfi, M. Rusciadelli, and V. Scisciani, 1998, Il buttressing delle faglie sinsedimentarie pre-thristing sulla strutturazione neogenica della catena appenninica: l'esempio della montagna dei fiori (Appennino central esterno): Bollettino della Società Geologica Italiana, **117**, 725–745.

Cattaneo, M., P. Augliera, G. De Luca, A. Gorini, A. Govoni, S. Marcucci, A. Michelini, G. Monachesi, D. Spallarossa, L. Trojani, and XGUMS, 2000, The 1997 Umbria-Marche (Italy) earthquake sequence: Analysis of the data recorded by the local and temporary networks: Journal of Seismology, **4**, no. 4, 401–414.

Chiarabba, C., and A. Amato, 2003, Vp and Vp/Vs images in the Mw 6.0 Colfiorito fault region (central Italy): A contribution to the understanding of seismotectonic and seismogenic processes: Journal of Geophysical Research, **108**, B5, doi: 10.1029/2001JB001665.

Chiaraluce, L., M. R. Barchi, C. Collettini, F. Mirabella, and S. Pucci, 2005, Connecting seismically active normal faults with Quaternary geologic structures: The Colfiorito 1997 case history (northern Apennines, Italy): Tectonics, **24**, TC1002, doi: 10.1029/2004TC001627.

Chiaraluce, L., W. L. Ellsworth, C. Chiarabba, and M. Cocco, 2003, Imaging the complexity of an active complex normal fault system: The 1997 Colfiorito (central Italy) case study: Journal of Geophysical Research, **108**, doi: 10.1029/2002JB002166.

Cinti, F. R., L. Cucci, F. Marra, and P. Montone, 2000, The 1997 Umbria-Marche earthquakes (Italy): Relation between the surface tectonic breaks and the area of deformation: Journal of Seismology, **4**, 333–343.

Collettini, C., and M. R. Barchi, 2002, A low angle normal fault in the Umbria region (central Italy): A mechanical model for the related microseismicity: Tectonophysics, **359**, 97–115.

Collettini, C., M. R. Barchi, L. Chiaraluce, F. Mirabella, and S. Pucci, 2003, The Gubbio fault: Can different methods give pictures of the same object?: Journal of Geodynamics, **36**, 51–66.

Coltorti, M., A. Albianelli, A. Bertini, G. Ficcarelli, M. Laurenzi, G. Napoleone, and D. Torre, 1998, The Collecurti mammal site in the Colfiorito area (Umbro-Marchean Apennine, Italy): Geomorphology, stratigraphy, paleomagnetism and palynology: Quaternary International, **47**, no. 8, 107–116.

CPTI, Working Group, 1999, Catalogo Parametrico dei Terremoti Italiani: Produced jointly by Istituto Nazionale di Geofisico, Gruppo Nazionale per la Difesa dai Terremoti, Storia Geofisica Ambiente, and Servizio Sismico Nazionale.

Cresta, S., S. Monechi, and G. Parisi, 1989, Stratigrafia del mesozoico e cenozoico nell'area umbro-marchigiana. Itinerari geologici sull'Appennino Umbro-Marchigiano (Italia): Memorie Descrittive della Carta Geologica d'Italia 39.

Deschamps, A., F. Courboulex, S. Gaffet, A. Lomax, J. Virieux, A. Amato, A. Azzara, B. Castello, C. Chiarabba, G. B. Cimini, et al., 2000, Spatio-temporal distribution of seismic activity during the Umbria-Marche crisis, 1997: Journal of Seismology, **4**, no. 4, 377–386.

Deschamps, A., G. Innaccone, and R. Scarpa, 1984, The Umbrian earthquake (Italy) of 19 September 1979: Annales Geophysicae, **2**, no. 1, 29–36.

Dziewonski, A. M., J. E. Franzen, and J. H. Woodhouse, 1985, Centroid-moment tensor solutions for April–June, 1984: Physics of the Earth and Planetary Interiors, **37**, 87–96.

Ekström, G., A. Morelli, E. Boschi, and A. M. Dziewonski, 1998, Moment tensor analysis of the central Italy earthquake sequence of September-October 1997: Geophysical Research Letters, **25**, 1971–1974.

Elter, P., G. Giglia, M. Tongiorgi, and L. Trevisan, 1975, Tensional and compressional areas in the recent (Tortonian to Present) evolution of the northern Apennines: Bollettino di Geofisica Teoricaed Applicata, **17**, 3–18.

Ficcarelli, G., and P. Mazza, 1990, New fossil findings from the Colfiorito basin (Umbro-Marchean Apennine): Bollettino Società Paleontologica Italiana, **29**, 245–247.

Gray, S. H., J. Etgen, J. Dellinger, and D. Whitmore, 2001, Seismic migration problems and solutions: Geophysics, **66**, 1622–1640.

Haessler, H., R. Gaulon, L. Rivera, R. Console, M. Frogneux, G. Gasparini, L. Martel, G. Patau, M. Siciliano, and A. Cisternas, 1988, The

Perugia (Italy) earthquake of 29 April 1984: A microearthquake survey: Bulletin of the Seismological Society of America, **78**, 1948–1964.
Kissling, E., W. L. Ellsworth, D. Eberhart-Phillips, and U. Kradolfer, 1994, Initial reference models in local earthquake tomography: Journal of Geophysical Research, **99**, 19635–19646.
Klein, F. W., 1989, User's guide to HYPOINVERSE, a program for VAX computers to solve earthquake locations and magnitudes: U. S. Geologic Survey Open-File Report 89–314.
Lavecchia, G., F. Brozzetti, M. Barchi, M. Menichetti, and J. V. A. Keller, 1994, Seismotectonic zoning in east-central Italy deduced from an analysis of the Neogene to Present deformations and related stress fields: Geologic Society of America Bulletin, **106**, 1107–1120.
Mariucci, M. T., A. Amato, and P. Montone, 1999, Recent tectonic evolution and present stress in the northern Apennines (Italy): Tectonics, **18**, 108–118.
Martinis, B., and M. Pieri, 1964, Alcune notizie sulla formazione evaporitica dell'Italia centrale e meridionale: Memorie Società Geologica Italiana, **4**, 649–678.
Mazzotti, A., E. Stucchi, G. L. Fradelizio, L. Zanzi, and P. Scandone, 2000, Seismic exploration in complex terrains: A processing experience in the southern Apennines: Geophysics, **65**, 1402–1417.
Meghraoui, M., V. Bosi, and T. Camelbeeck, 1999, Fault fragment control in the Umbria-Marche, central Italy, earthquake sequence: Geophysical Research Letters, **26**, 1069–1072.
Messina, P., F. Galadini, P. Galli, and A. Sposato, 1999, Evoluzione a lungo termine e caratteristiche della tettonica attiva nell'area umbro-marchigiana colpita dalla sequenza sismica del 1997-98 (Italia centrale), *in* L. Peruzza, ed., Progetto MISHA — Metodi innovativi per la stima dell'hazard: applicazione all'Italia centrale: Centro Nazionale delle Ricerche-Gruppo Nationale per la Difesa dai Terremoti, 32–42.
Miller, S. A., C. Collettini, L. Chiaraluce, M. Cocco, M. Barchi, and B. J. P. Kaus, 2004, Aftershocks driven by a high-pressure CO_2 source at depth: Nature, **427**, 724–727.
Mirabella, F., and S. Pucci, 2002, Integration of geologic and geophysical data along a section crossing the region of the 1997–98 Umbria-Marche earthquake (Italy): Bollettino della Società Geologica Italiana special volume 1, 891–900.
Mirabella, F., V. Boccali, and M. R. Barchi, 2005, Segmentation and interaction of normal faults within the Colfiorito fault system (central Italy), *in* D. Gapais, J. P. Brun, and P. R. Cobbold, eds., Deformation mechanisms, rheology and tectonics: From minerals to the lithosphere: Geologic Society of London special publication 243, 25–36.
Mirabella, F., M. G. Ciaccio, M. R. Barchi, and S. Merlini, 2004, The Gubbio fault (central Italy): Geometry, displacement distribution and tectonic evolution: Journal of Structural Geology, **26**, 2233–2249.
Olivieri, M., and G. Ekström, 1999, Rupture depths and source processes of the 1997–1998 earthquake sequence in central Italy: Bulletin of the Seismological Society of America, **89**, 305–310.
Pauselli, C., R. Marchesi, and M. Barchi, 2002, Seismic image of the compressional and extensional structures in the Gubbio area (Umbrian-Pre-Apennines): Bollettino della Società Geologica Italiana special volume 1, 263–272.
Pialli, G., M. Barchi, and G. Minelli, eds., 1998, Results of the CROP03 deep seismic reflection profile: Memorie Società Geologica Italiana 52.
Pino, N. A., and S. Mazza, 1999, Rupture directivity of the major shocks in the 1997 Umbria-Marche (central Italy) sequence from regional broadband waveforms: Geophysical Research Letters, **26**, 2101–2104.
Pizzi, A., and V. Scisciani, 2000, Methods for determining Pleistocene-Holocene displacement in active faults reactivating pre-Quaternary structures: Example from the central Apennines (Italy): Journal of Geodynamics, **29**, 445–457.
Pizzi, A., F. Calamita, M. Coltorti, and P. Pieruccini, 2002, Quaternary normal faults, intramontane basins and seismicity in the Umbria-Marche-Abruzzi Apennine ridge (Italy): Contribution of neotectonic analysis to seismic hazard assessment: Bollettino della Società Geologica Italiana special volume 1, 923–929.
Robein, E., 2003, Velocities, time-imaging and depth-imaging: Principles and methods, EAGE Publications.
Selvaggi, G., A. Deschamps, M. Ripepe, and B. Castello, 2002, Waveforms, arrival times, and locations of the 1997 Colfiorito (Umbria-Marche, central Italy) aftershocks sequence: Quaderni di Geofisica vol. 21.
Stramondo, S., M. Tesauro, P. Briole, E. Sansosti, S. Salvi, R. Lanari, M. Anzidei, P. Baldi, G. Fornaro, A. Avallone, et al., 1999, The September 26, 1997 Colfiorito, Italy, earthquakes: Modeled coseismic surface displacement from SAR interferometry and GPS: Geophysical Research Letters, **26**, 883–886.
Tavarnelli, E., 1999, Normal faults in thrust sheets: Pre-orogenic extension, post-orogenic extension or both?: Journal of Structural Geology, **21**, 1001–1018.
Wang, C. Y., 2002, Detection of a recent earthquake fault by the shallow reflection seismic method: Geophysics, **67**, 1465–1473.
Wessel, P., and W. H. F. Smith, 1995, New version of the generic mapping tools released: EOS, Transactions of the American Geophysical Union, **76**, 329.
Williams, R. A., J. K. Odum, T. L. Pratt, K. M. Shedlock, and W. J. Stephenson, 1995, Seismic surveys assess earthquake hazard in the New Madrid area: The Leading Edge, **14**, 30–34.
Yilmaz, O., 1988, Seismic data processing: SEG.
Yokokura, T., 1999, Seismic investigation of an active fault off Kobe: Another disaster in the making?: The Leading Edge, **18**, 1417–1421.
Zanzi, L., 1996, The WIM method for refraction statics: Geophysics, **61**, 1859–1870.